Sensors & Transducers, Vol. 25, Special Issue, December 2013, pp. 189-196

www.sensorsportal.com

Sensors & Transducers

© 2013 by IFSA

http://www.sensorsportal.com

Design and Algorithm Research of High Speed Two-wheeled Mini Robots

[1*] Jianzhong Wu, [2] Jianping Cai, [3] Linghui Fan, [2] Meimei Huo, [2] Zengwei Zheng

[1,2] Department of Computer Science, Zhejiang University City College, Hangzhou, 310015, China
[3] Ningbo Sunrun Electronic Information Technology Development Co. Ltd., Ningbo, 315211, China
[*] Tel.: 008657188015338, fax: 008657188015338
E-mail: wujianzhong@zucc.edu.cn

Received: 16 December 2013 /Accepted: 15 October 2013 /Published: 23 December 2013

Abstract: The IEEE Maze Micromouse is a kind of mini wheeled robot which has the features of automatic moving and path tracking in a standard maze. The Micromouse would record the track and calculate the best path according to intelligent algorithm and sprint to the end point. The structure and algorithm of a high speed DC motor are presented in this paper. A gesture calibration and fast search algorithm is advanced according to the high speed DC motor, acceleration sensors, gyroscopes and other parts. The experiments and simulation verified the advantages and promotions to the performance of Micromouse, which is helpful to achieve better score in maze competitions. *Copyright © 2013 IFSA.*

Keywords: Mini robot, Maze, Posture calibration, Hardware and software co-design.

1. Introduction

The Micromouse is a smart mini robot which equips with microcontroller, sensors and electromechanical moving parts. It can memory and select the path lane run automatically in a IEEE standard maze, looking for exit, and eventually reach the set destination which is on the center of the maze.

This kind of micro-robot maze game activities initiated in 1972 by the American Society of Mechanical magazine, and the original game devices are spring driven way. In 1977, the IEEE Spectrum magazine raised the concept of a Micromouse: Micromouse is a miniature robotic vehicle which has abilities of decoding and navigation, and controlled by a microprocessor in a complex maze.

The first Micromouse maze contest held in New York In 1979, and there was a rapid increasing to other countries after that [1]. The International Electrical and Electronic Engineers (IEEE) named it IEEE Standard Micromouse Maze Contest in 2006, and developed competition rules then [2]. Nowadays, IEEE holds international Micromouse maze competition annually which attracts colleges and universities students from all over the world to participate in them.

IEEE Micromouse Maze Contest is a competition with challenging, interesting but a certain degree of difficulty as well. Micromouse is a mini robot which combines various engineering knowledge together. Problems must be considerate including electronic, electrical, mechanical and control aspects. Other important factors such as weight, speed, power consumption, sensors, the center of gravity, algorithm programming should be concerned as well in a Micromouse design procedure.

Micromouse technology has a close relationship with various disciplines. The precise positioning capability, fast walking ability and excellent obstacle avoidance ability are necessary to a Micromouse. It could also be extended to more robot applications such as the design of industrial robots and special purpose robots. Meanwhile, the related technologies could be involved in the various disciplines of knowledge and can be applied in all relevant areas, respectively.

There is a long history with the Micromouse competition all around the world. With the continuously improvement on the hardware structure and software algorithms, competition teams have received good score records and made progress steady in the IEEE competitions of recent years. DC motors have been widely adopted because there high speed and celerity responsibility [3-5].

This paper analyzes the main technologies which relate to Micromouse performance. The drive mechanism, obstacle detection, walking speed, posture calibration algorithm and search algorithm are all introduced respectively [6]. Better applying and designing to the above Micromouse technologies provide supporting to achieve better scores in IEEE standard competitions [7-8].

The rest of the paper demonstrates the whole hardware structure and software architecture of a newly designed Micromouse. Section 2 introduce the overview of the Micromouse design; The mechanic, IR detection and motor technologies are presented in section 3; Section 4 introduce the Micromouse co-design of software and hardware; Simulation tests and results are presented in section 5; Finally section 6 is the conclusion part of this paper.

2. Design Overview

2.1 Basic Framework of Micromouse

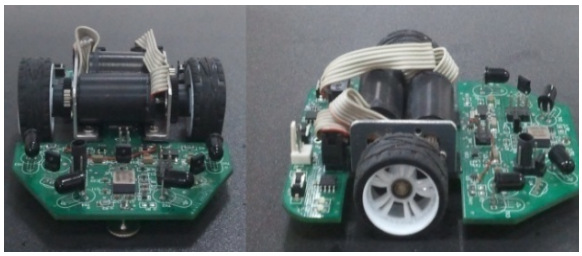

Fig. 1. High speed DC motor Micromouse.

The Micromouse is a mini robot with intelligent features. The main parts of a Micromouse including the microprocessor, walking parts detection components, attitude stabilization components, power supply parts and human-computer interaction components [9-11]. Fig. 1 shows the physical Micromouse photo of a high speed Micromouse and Fig. 2 shows its system structure.

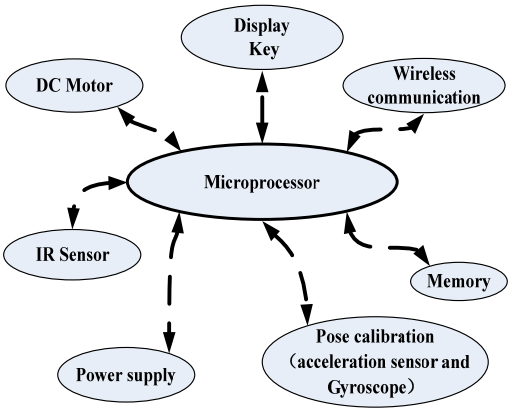

Fig. 2. Schematic diagram of the mother control board.

2.2. Key Components Requirements

2.2.1. Motor Parameters

The walking performance including speed, stability and breaking, are mainly rely on the motors, which like feet of a Micromouse.

2 kinds of typical motors are selectable, DC motor and stepper motor. Stepper motor has a relatively simpler speed but easy to control, while the DC motor has high speed, simple driver circuit but complex in programming.

More work should be done to ensure a high speed, stability, meanwhile, a speed measuring devices is necessary to realize a good speed control loop.

2.2.2. Linear Infrared Sensor

Obstacle detection is the ability that a Micromouse avoids collision in the maze when walking in it.

The common detect sensors including infrared, ultrasonic, laser and camera in Micromouse design.

According the experiences and analysis of work ahead, infrared has excellent linearity to light intensity and is able to detect infrared reflected light between 2 cm to 50 cm with high accuracy.

2.2.3. Acceleration Sensor and Gyroscope

There is poses balancing problem with a moving objects. The Micromouse is also troubled with the posture calibration during a high speed running in the maze.

The acceleration sensor and gyroscope should have a stable and a wide range of angular velocity detection capability to the walking optimization of a Micromouse. With helps of the 2 type of sensors and optimize algorithm, a Micromouse could finish posture calibration and rotation perception.

This perception of the state of the Micromouse, intelligent algorithm, complete attitude adjustment and rotation perception.

3. Optical, Mechanical and Electrical Design

3.1. Motor Characters

The DC motor EN1524 006SR with encoder IE2-512 of FAULHABER are adopted according to the requirements of the DC motor. The working voltage is 6 V, torque is 12 Ncm, the speed is 9700 rpm and the speed coefficient is 1650 rpm/V. The accuracy of the encoder is 512 lines per revolution.

The motor operating voltage 6 V, 12 Ncm of torque, speed 9700 rpm speed coefficient 1650 rpm/V.

These incremental shaft encoders in combination with the DC-Micromotors and brushless DC-Servomotors are used for indication and control of both, shaft velocity and direction of rotation as well as for positioning.

The encoder is integrated in the DC-Micromotors and extends the overall length by only 1.4 mm and build-up option for DC-Micromotors and brushless DC-Servomotors.

Hybrid circuits with sensors and a low inertia magnetic disc provide two channels with 90° phase shift.

The supply voltage for the encoder and the DC-Micromotor as well as the two channel output signals are interfaced through a ribbon cable with connector.

3.2. Wheel Drive and Gear Engaging

The Micromouse has compact characteristic with DC motor. The weight is less than 100 g.

The Mechanical parts mainly constitute by the gear, wheels and mounting bracket. Fig. 3 is the 3-side views of the DC motor Micromouse.

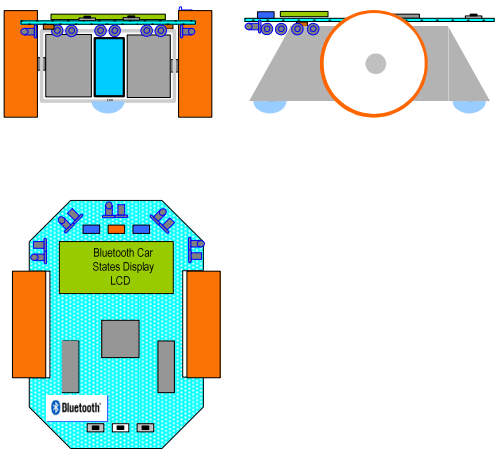

Fig. 3. 3-side views of the DC motor Micromouse.

The constant speed of DC motor is 9700 rpm. The PWM adjust the motor speed to 2000 rpm, and then the power transmitted to the wheels through the speed reduction gear. Suppose that the required maximum sprint speed is 200 cm / s, when using a wheel diameter of 28 mm, than the rotational speed of the wheel is:

$$\frac{2000*60}{28*2\pi} \approx 682\ rpm$$

The reduce rate is:

$$2000:682 \approx 45:15$$

The parameters of gear and motor are available according to the calculated above. The motor gear parameters is M0.3 × 15T, and the transmission gears parameter is M0.3 × 45T, the gear having a thickness of 2.5 mm, the material is POM for lightweight consideration.

The accurate design of the robot frame is essential important to achieve a precise engagement to ensure a reliable power transmission between the motor gear and the wheel drive gear.

Too tight and too loose engagement should be both avoided, the tight engagement would lead to induced torque losses, while too loose would bring large noise and even difficult driving.

The diameter of motor is 15 mm, the shaft diameter is 2 mm and the spacing between motor and shaft is 1mm, then:

Gears center distance = modulus * (small gear + large gear) / 2 = 0.3 × (45 +15) / 2 = 9 mm

The maximum diameter of motor gear is 5.1 mm:

0.3 × (15 +2) = 5.1 mm

So the frame structure size is determined and shown in Fig. 4.

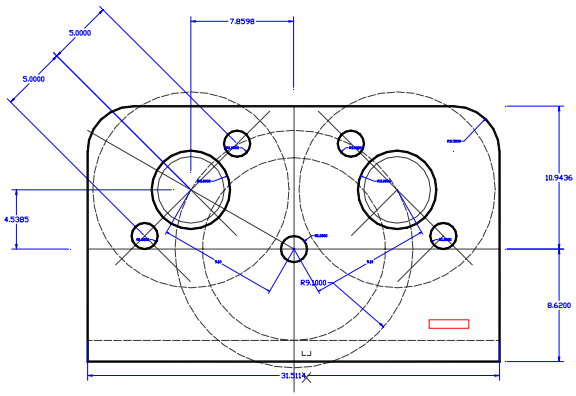

Fig. 4. DC motor frame layout.

3.3. Linear Infrared Scanning Ranging

The infrared sensor distance measurement is a commonly used method, which measures distance convert the value of receive sensor to a distance from the reflect surface.

The method presented in this paper is an optimized one comparing the common one, which is

also an application to the principle of the reflective infrared sensor to detect obstacles.

The transmitters and the receivers are coupled equipped on the front and 45-degree direction, each receiver could receive infrared signal reflect from the surface which is sent by the coupled transmitter only.

At the same time, the reflect signal could be detect only if the distance of obstacle is within the effective distance, otherwise, it can't be detected.

The infrared transmitter model adopted in this design is IR7393C, the specifications are as the following: 8.4 mW maximum output power, 60° maximum radiation angle, 940 nm operating wavelength; the receiver model is TSL262R which has an operating wavelength (most sensitive) of 940 nm, and has a good linearity in effective area.

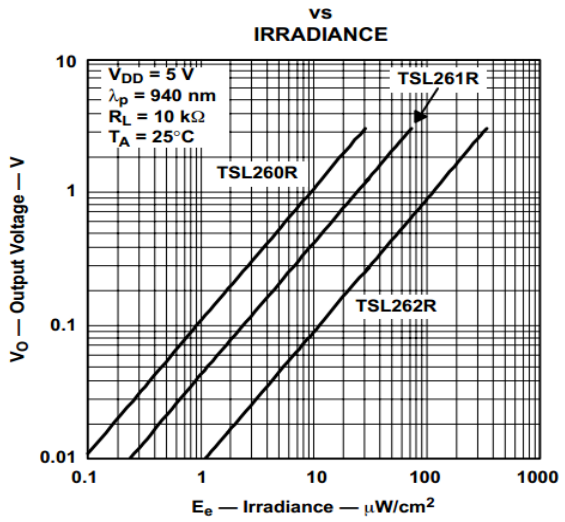

Fig. 5. The relationship of lightness and output power.

The received signal is converted to distance value after A/D conversion, filtering and fitting process.

3.4. Acceleration Sensors and Gyroscopes Error Factors

An acceleration sensor can be used to measure the acceleration.

The acceleration sensor measures only the acceleration of gravity under fixed speed (constant linear motion), or still state.

The acceleration of gravity is corresponding to the absolute coordinate system, so the angle offset between the sensor and the ground coordinate system is available from the output of acceleration sensor.

Gyroscope can be used to measure angular velocity. It has high dynamic characteristics. But it is an indirect measurement device because the output result is a derivative of the angle (angular velocity). Obviously it is necessary to integral the angel velocity to get the angle value, which there is a fatal integral error problem.

Temperature compensation calibration should be considerate thoroughly because temperature changes always leading to a compensation calibration.

It is common practice to temperature-calibrate gyros to improve their overall accuracy. The ADXRS610 has a temperature proportional voltage output that provides input to such a calibration method [12]. The temperature sensor structure is shown in Fig. 6. The temperature output is characteristically nonlinear, and any load resistance connected to the TEMP output results in decreasing the TEMP output and temperature coefficient. Therefore, buffering the output is recommended.

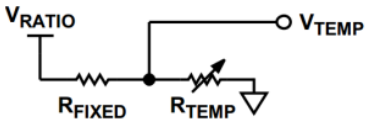

Fig. 6. ADXRS610 Temperature Sensor Structure.

3.5. Wheels Anti-skid Research

When the Micromouse runs at high speed in the maze, the friction between the wheels and the maze floor must be bigger enough to anti-skid which would lead to a calculate error or even collision with the maze wall. Friction is particularly critical especially in the turns. Natural rubber (NR) is selected as the wheel rubber to increase friction.

4. Hardware and Software Co-design

4.1. Distance Measurement Fitting Algorithm

The relationship between the distance and the voltage is available based on the infrared light intensity reflection principle:

$$r = 10^{(\log V_0 - d)/c} \quad (1)$$

Formula (1) gives the corresponding relationship of r and V_0. The coefficients c and d could be determined with two groups of r and V_0 according to the formula.

Then, the linear relationship between distance and infrared sensor within the effective range is available according to the formula (1) and Fig. 5. A table is prepared to fill the signal voltage and the corresponding distance value which is helpful to greatly decrease the calculate operation amount of processor, but it would produce a tiny error in conversion a voltage which is not in the table, anyway, it could be ignored.

The accuracy distance could be available only if the coefficients c and d are accurately obtained. The coefficients of each group of infrared should be measured twice to ensure their measuring precision.

4.2. Posture Calibration Algorithm

The accuracy of acceleration sensor is stable and the variation of the measured values over time is relatively small but is easily affected by external interference.

The angular offset can be integrated with the gyroscope, which has good dynamic performance and is not subject to external interference, but the integral cumulated error would affect the measuring distance. In total, regardless of how long would the acceleration sensor work, it would be hard to be affected by external interference, and the measurement results are always accurate!

The gyroscope is not subject to external interference, but over time, accumulated integration error would increase measurement error.

The new algorithm is to balance the output results of the two sensors, which is to set different weights in different periods to produce a more accuracy angle value. That is, increasing the weight of gyroscope result output in short period while increasing the weight of acceleration result output in long period.

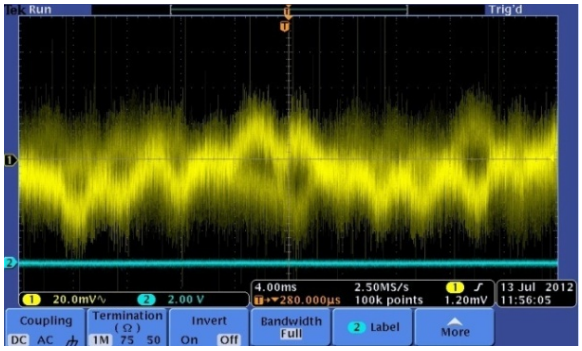

Fig. 7. Gyroscope output signal when the motor operating.

According to the analysis above, Kalman filter algorithm is used as the basic algorithm (The Kalman Filter Algorithm, KM). Firstly, the state and measurement equations of system are established. The angular velocity is the derivative of the angle, and the actual angle φ is used as the state vector [13].

In this algorithm, the office b of gyro is estimated by acceleration sensor, this offset is set as the state vector to obtain the corresponding state and measurement equations:

$$\begin{bmatrix} \dot{\phi} \\ \dot{b} \end{bmatrix} = \begin{bmatrix} 0 & -1 \\ 0 & 0 \end{bmatrix} \begin{bmatrix} \phi \\ b \end{bmatrix} + \begin{bmatrix} 1 \\ 0 \end{bmatrix} \omega_G + \begin{bmatrix} \omega_g \\ 0 \end{bmatrix} \tag{2}$$

$$\phi_A = \begin{bmatrix} 1 & 0 \end{bmatrix} \begin{bmatrix} \phi \\ b \end{bmatrix} + \omega_a$$

In Formula (2), ϕ_A is the angle values obtained after treatment from the acceleration sensor; ω_G is the angular velocity output from the gyro output which contains the fixed deviation; ω_g is the gyroscope measurement drift values; ω_a is the acceleration sensor votes shift values; b is the gyroscope drift errors. ω_g and ω_a are independent with each other.

After transforming, the optimum estimate and covariance in state k is available as following:

$$X(k|k) = X(k|k-1) + K(k)(Z(k) - HZ(k|k-1))$$

$$P(k|k) = (I - Kg(k)H)P(k|k-1)$$

Wherein: K is the Kalman Gain, I is a unit matrix.

By calculating to above equation in cycle, the best results are available [14].

Constantly clearing the diminishing integral quantities in accelerate direction is the core of the fusion algorithm.

In order to run the program on a general purpose processor, it is possible not to explicitly calculate the attitude angle, but only output the corrected signal to control the motor as feedback. The advantage is the operation could be simply finished with integer type.

If there is a high-performance processor, explicitly solving attitude Kalman filtering could be implemented. Kalman filtering also process with the historical data points, and synchronizes to the integration of the gyroscope and acceleration data, gyroscope and acceleration contribution weights can also be adjusted through the filter parameters [15-18].

4.3. Maze Search Algorithm

A partition to heart optimization algorithm is designed through the researching of maze search algorithm of a Micromouse.

The thinking of the partition to heart algorithm is shown in Fig. 8, the maze is divided into 12 regions beside the end point, and the Micromouse would walk along the direction of the closest to the maze center. While within the separate region, the similar potential value algorithm would be implemented i.e. indifferent regions, the Micromouse would walk along the current absolute direction to choose the discipline of most near to the center point, then set one of the 4 rules of right hand, left hand, center right hand and center left hand as the implemented rule to explore the shortest path in the maze.

For example, when the Micromouse is in partition 7, if its absolute direction is toward the north, right-hand rule is the rules of the closest one to the end point; while the Micromouse has an absolute direction of toward the east, center-left rule is the best one to the end point; similarly, while the Micromouse' absolute direction is toward the south, left-hand rule is the best one to the end point; while

the Micromouse's absolute direction is toward the west, right-hand rule is the best one. Walking rules of other partitions are shown in Fig. 9. From the description above the Fig. 9, the Partition to central algorithm is more central-trend than other algorithms.

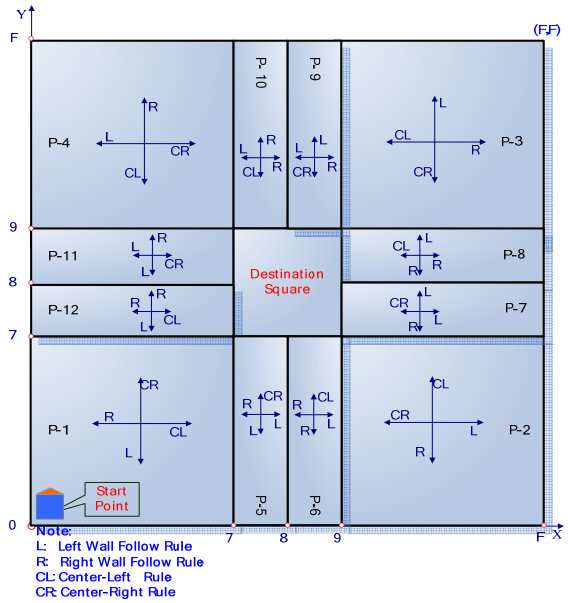

Fig. 8. Partition to center algorithm.

In Fig. 8, the arrows point to the possible direction when the Micromouse is in this partition cells. The letter represents the available rule for choosing.

Fig. 9 shows the algorithm flow chart.

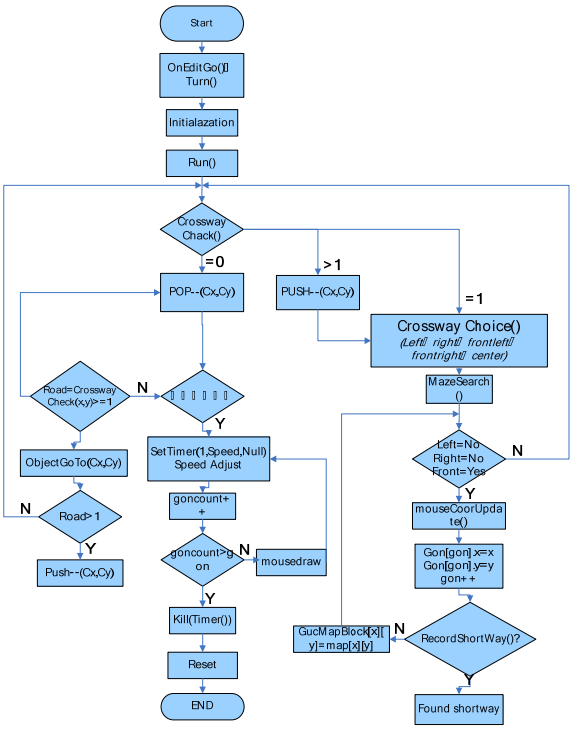

Fig. 9. Simulator Structure Flowchart.

4.4. Others

4.4.1. Detection Strategy

There are 2 detection strategies in Micromouse maze walk. The first one is whole maze exploration. A Micromouse would explore all maze units to find out the best walking path. The disadvantages are the need to have sufficient time or number of detection times and low efficiency. The second strategy is partial exploration, i.e. to find out the best path in the limited time or detection times.

4.4.2. Sprint Algorithm

Sprint algorithm is implemented when a Micromouse back to the start point, which calculates the shortest path of the maze after exploration. The Micromouse would walk along the shortest path to until to the end. In the sprint process, the Micromouse would speed up on straights lane, and strive to reach the finish line in the shortest time.

5. Simulation Test

5.1. Linear Infrared Sensor Test

Table 1 verifies the accuracy of the conversion of infrared test. The method is to accurately measure the distance value within the range of 60 mm to 180 mm with a ruler, then put the Micromouse on the same location respectively to read the distance which is converted from the current infrared voltage value.

Table 1. Verification of infrared process.

Supposed (cm)	6	7	8	9	10	11	12
IR voltage (mV)	1610	1277	1021	887	770	663	589
Converted distance (cm)	60.0	71.0	82.0	92.0	10.2	11.4	12.5
Supposed (cm)	13	14	15	16	17	18	-
IR voltage (mV)	529	486	448	416	387	354	-
Converted distance (cm)	13.4	14.5	15.2	16.1	17.0	18.0	-

We can see the maximum error between the infrared converted distance and the ruler measured distance is 5mm form the verification table above. The 5 mm error is not interested in a Micromouse produced large offset; moreover, it can be further corrected by software algorithms.

5.2. Fusion Algorithm Verification

Tests of enabling the Kalman filtering algorithm and disabling were made to verification the efficiency of algorithm. The time lasted 10 minutes when

putting the Micromouse on the maze board. The tests result is show on Fig. 10.

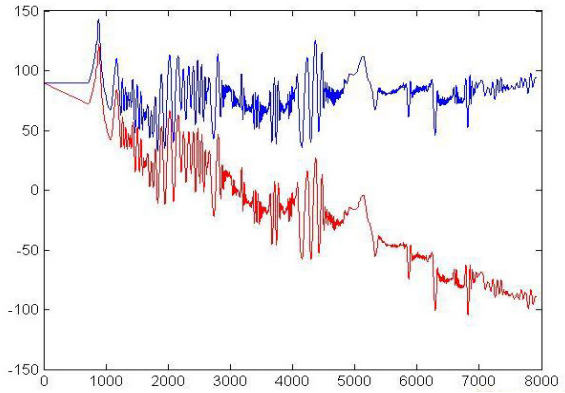

Fig. 10. Kalman algorithm verification.

The blue curve shows the angle value processed with the Kalman filter algorithm while the red curve shows the angle value which is not processed with the algorithm. It is easy to see that the Kalman filter algorithm could eliminate the accumulated error produced by the gyroscope.

5.3. Turning Verification

Firstly, marking the turning test with gesture calibration as Test A and turning test without gesture calibration as Test B. Secondly, programming the 2 algorithms to the Micromouse and turning the mode onto continuous testing. Thirdly, put the Micromouse on the maze board. The Micromouse would start the turning test and it would run a 360 ° turning program with algorithm A and pause for 3 seconds then run a 360° turning program with algorithm B, then go to another circle. The actual angle should be recorded on each test. 10 tests results curves of both algorithm are both shown on Fig. 11, the results show that accuracy promoted 42.71 % with gesture calibration algorithm.

5.4. Accelerate Algorithm

16 times of speed switching were simulated and the speed values were recorded in the study. The relationship of speed and time was demonstrated in curve with the Matlab. The red curve in Fig. 12 is the curve of 300cm/s acceleration which is calculated accurate curve, while the blue curve is the calculated speed curve.

5.5. Smooth Turning Test

The speed difference of two motors is used to realize smooth turn algorithm when walk in the lane of maze. The correction value must be calculated before to decide the angles to turn for the left and right motors.

There are a linear relationship between speed and the offset in turning process, so the offset (the distance measured by the left and right infrared sensors) could be used by MCU to calculate the correction rate and decide different speed values to the two motors. The smooth turning algorithm greatly simplifies the complexity of the infrared range and motor control.

The prerequisite of the way is that the infrared distance measuring process must be finished accurately and quickly, otherwise the amendment process would have a delay which would directly result in a hitting on the maze board.

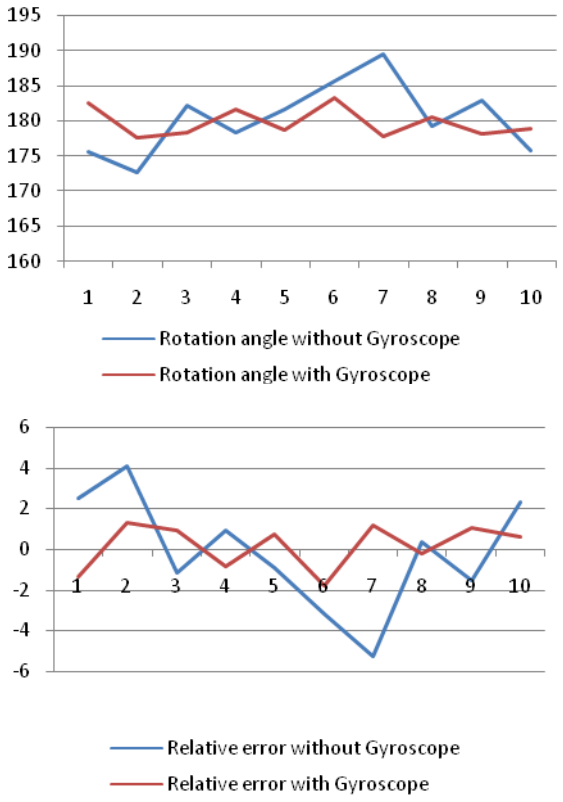

Fig. 11. Posture calibration algorithm test.

5.6. Maze Exploring Test and Verification

In order to test and validate the advantages of the algorithm, some typical game of mazes are selected. The verification results with mazes of competition UK, LW, ST, TI, KATO and Beijing are lists in Table 2.

Table 2 shows: there is big difference in efficiency performance with the same algorithm in different maze; meanwhile, there is also big difference in efficiency performance with difference algorithms putting on the same maze. Distinctly, the partition to center algorithm has great advantages in exploring efficiency in most of mazes.

Table 2. A comparison of the Exploring Steps and Shortest Path Steps.

Rules	Steps	UK	LW	ST	TI	KATO	BJ
Left Wall Following	**Shortest Path**	41	-	47	37	73	135
	Exploring	261	-	311	259	147	135
Center-Left	**Shortest**	41	71	47	37	63	73
	Exploring	367	277	351	315	181	205
Central	**Shortest**	41	71	47	37	63	73
	Exploring	141	299	109	61	293	113
Partition-Central	**Shortest Path**	41	71	47	37	63	73
	Exploring	169	135	91	61	171	113

6. Conclusion

The design and algorithms of a dual wheel mini robot is presented in this paper. It equipped with an acceleration sensor, a gyroscope, and DC motors and infrared sensors are adopted.

With assistance of the new calibration algorithm and search algorithms, the performance of the mini robot has been promoted a lot than a normal Micromouse without the optimize algorithm. According the experiments and simulations above, the total speed and performance promotion is near 50 %. Meanwhile, there is a 30 % average reducing with the new maze searching algorithm compare to the traditional algorithms.

Acknowledgments

The authors gratefully acknowledge the support of Zhejiang Provincial Education Department 2012 project No JB170, the Science Foundation of Zhejiang Province innovation teams project No 2010R50009, the Key Lab.Mob.Net.App.Tech of Zhejiang Director project No 2010E10005.

This work has been supported by Hangzhou Key Laboratory for IoT Technology & Application.

References

[1]. Micromouse competition, *Electronic Systems News*, No. 1, 1987, pp. 45.

[2]. Provo, B., How they do it in Singapore: New Zealand Micromouse, *Association Newsletter*, 1991, pp. 5.

[3]. M. Chiodo, Hardware-Software Co-Design of Embedded Systems, *IEEE Micro*, No. 8, 1995, pp. 26-36.

[4]. Sharma M., Robeonics K., Algorithms for Micro-mouse, *Future Computer and Communication 2009*, Vol., No., 2009, pp. 581-585.

[5]. Sadik A. M. J., Dhali M. A., Farid H. M. A. B., Rashid T. U., Syeed, A., A Comprehensive and Comparative Study of Maze-Solving Techniques by Implementing Graph Theory, *Artificial Intelligence and Computational Intelligence,* 2010. pp. 52-56.

[6]. Kibler S. G., Hauer A. E., Giessel D. S., Malveaux C. S., Raskovic D., *IEEE Micromouse for Mechatronics research and education, Mechatronics*, 2011, pp. 887-892.

[7]. Jiang Xiangtao, Xin Dongjun, Wu Guangwei, Jiang Xing, The Platform Design that Simulates the Micromouse Move in the Maze, *Intelligent System Design and Engineering Application,* 2012, pp. 1152-1155.

[8]. Matthews T. W., Spencer R. R., An autonomous race car design competition, *IEEE Trans. on Education*, No. 2, 2011, pp. 9-10.

[9]. Phan Anh Tuan, Hydrodynamics of Autonomous Underwater Vehicles, *Journal of Mechatronics*, Vol. 1, No. 1, 2012, pp. 25-28.

[10]. Irfan Ullah, Qurban Ullah, Furqan Ullah, Seoyong Shin, Sensor-Based Autonomous Robot Navigation with Distance Control, *Journal of Computational Intelligence and Electronic Systems,* Vol. 1, No. 2, 2012, pp. 161-168.

[11]. Irfan Ullah, Furqan Ullah, Qurban Ullah, Seoyong Shin, Object Following Fuzzy Controller for a Mobile Robot, *Journal of Computational Intelligence and Electronic Systems,* Vol. 1, No. 1, 2012, pp. 86-90.

[12]. ADXRS610 ±300°/s Yaw Rate Gyro Data Sheet, www.sparkfun.com/datasheets/Sensors/ADXRS610.pdf

[13]. Feng Zhiyong, Zeng Han, Zhang Li, Zhao Yixin Huang Wei, Angle Measurement Based on Gyroscope and Accelerometer Signal Fusion, *Journal of Southwest China Normal University,* Vol. 36, No. 4, 2011, pp. 137-141:.

[14]. Kalman R. E., A New Approach to Linear Filtering and Prediction Problems, *Transaction of the ASME-Journal of Basic Engineering*, No. 82, 1960, pp. 35-45.

[15]. Piyabongkarn D., Rajamani R., Greminger M., The development of a MEMS gyroscope for absolute angle measurement, *Control Systems Technology*, Vol. 13, No. 2, 2005, pp. 185-195.

[16]. Degani O., Seter D. J., Socher E., Kaldor S., Nemirovsky Y., Optimal design and noise consideration of micromachined vibrating rate gyroscope with modulated integrative differential optical sensing, *Journal of Microelectromechanical Systems,* Vol. 7, No. 3, 1998, pp. 329-338.

[17]. Wen Hong Zhu, Lamarche T., Velocity Estimation by Using Position and Acceleration Sensors, *IEEE Transactions on Industrial Electronics,* Vol. 54, No. 5, 2007, pp. 2706-2715.

[18]. JungKeun Lee, Park E. J., Robinovitch S. N., Estimation of Attitude and External Acceleration Using Inertial Sensor Measurement During Various Dynamic Conditions, *IEEE Transactions on Instrumentation and Measurement,* Vol. 61, No. 8, 2012, pp. 2262-2273.

2013 Copyright ©, International Frequency Sensor Association (IFSA). All rights reserved. (http://www.sensorsportal.com)